

CREEP AND FABRICS OF POLYCRYSTALLINE ICE UNDER SHEAR AND COMPRESSION

By PAUL DUVAL

(Laboratoire de Glaciologie, 2, rue Très-Cloîtres, 38031 Grenoble Cédex, France)

ABSTRACT. Creep tests were performed in torsion and torsion-compression on polycrystalline ice at temperatures near the melting point. Syntectonic recrystallization occurs at strains of the order of 2–3%, leading to a rapid increase in strain-rate. It is shown that the increase of creep-rate during tertiary creep arises from the development of fabrics favouring the glide on basal planes but also from the softening processes associated with recrystallization. The c -axis fabric of recrystallized ice developed in simple shear consists of two-maxima, one at the pole of the permanent shear plane and the other between the normal of the second plane of maximum shearing stress and the principal direction of compression. In torsion-compression, a three- or four-maximum fabric is formed according to the intensity of different components of the stress tensor. The maxima are clustered around the principal direction of compression. Processes of fabric formation are discussed. The experimentally developed fabrics are probably produced by the strain-induced recrystallization, for which the driving force is provided by differences in stored plastic strain energy. However the degree of preferred orientation of ice c -axes must be a function of the total strain when syntectonic recrystallization becomes less important. In this case, fabrics are principally formed by plastic flow and a steady state is obtained for very high strains.

RÉSUMÉ. *Fluage et recristallisation de la glace polycristalline soumise au cisaillement et la compression.* Des expériences de fluage ont été réalisées en torsion et torsion-compression sur de la glace polycristalline près du point de fusion. La recristallisation syntectonique débute pour des déformations de l'ordre de 2 à 3%, entraînant une augmentation rapide de la vitesse de déformation. On montre que l'augmentation de la vitesse du fluage durant le fluage tertiaire provient de la formation de fabriques qui favorise le glissement basal, mais aussi des processus d'adoucissement associés à la recristallisation. En cisaillement simple, les fabriques de la glace recristallisée consistent en deux maxima, dont l'un est confondu avec le pôle du plan de cisaillement permanent et l'autre est situé entre la normale au deuxième plan de cisaillement maximum et la direction principale de compression. En torsion-compression, des fabriques à trois ou quatre maxima sont formées suivant l'intensité des différentes composantes du tenseur des contraintes. Les maxima entourent dans tous les cas la direction principale de compression. On discute des processus de formation des fabriques. Les fabriques obtenues dans ces expériences sont probablement produites par la recristallisation dont le moteur est l'énergie de la déformation plastique. L'orientation préférentielle des axes c des cristaux de glace doit être une fonction de la déformation totale atteinte lorsque la recristallisation syntectonique devient moins importante. Dans ce cas, les fabriques sont principalement formées par la déformation plastique et un état permanent est obtenu seulement pour des déformations très importantes.

ZUSAMMENFASSUNG. *Kriechen und Gefüge polykristallinen Eises unter Scherung und Kompression.* Bei Temperaturen nahe dem Schmelzpunkt wurden Kriechversuche an polykristallinem Eis unter Torsion und Torsion-Kompression angestellt. Bei Deformationen der Größenordnung 2–3% tritt syntektonische Rekrystallisation auf, die zu einem raschen Anwachsen der Deformationsrate führt. Es wird gezeigt, dass die Zunahme der Kriechrate bei tertiärem Kriechen auf die Entwicklung eines Gefüges, das das Gleiten auf Basisebenen begünstigt, aber auch auf die mit der Rekrystallisation verbundenen Erweichungsprozesse zurückzuführen ist. Das c -Achsen-Gefüge rekristallisierten Eises, das sich unter einfacher Scherung entwickelt, weist zwei Maxima auf, eines am Pol der permanenten Scherfläche und das andere zwischen der Normalen auf die zweite Ebene maximaler Scherspannung und der Hauptrichtung der Kompression. Unter Torsion-Kompression bildet sich ein Gefüge mit drei oder vier Maxima, je nach der Intensität verschiedener Komponenten des Spannungstensors. Die Häufungsstellen der Maxima liegen um die Hauptrichtung der Kompression. Vorgänge bei der Gefügebildung werden diskutiert. Die experimentell erzeugten Gefüge entstehen vermutlich infolge der spannungsinduzierten Rekrystallisation, die ihre Triebkraft aus Unterschieden in der gespeicherten plastischen Verformungsenergie bezieht. Jedoch muss der Grad der bevorzugten Orientierung von c -Achsen im Eis eine Funktion der Gesamtverformung sein, wenn die syntektonische Rekrystallisation an Bedeutung verliert. In diesem Fall bildet sich das Gefüge vor allem durch plastisches Fließen und wird für sehr hohe Verformungen stationär.

INTRODUCTION

The plastic behaviour of polycrystalline ice has mostly been studied by carrying out creep tests using a constant load (Glen, 1955; Steinemann, 1958; Kamb, 1972). On the macroscopic scale, polycrystalline ice demonstrates a transient or primary creep whose rate diminishes with time, and subsequently a secondary creep in which the creep-rate is steady with time. If the load is applied for a long time, so that deformation exceeds two or three per cent strain, the creep-rate starts to accelerate and a new steady state (tertiary creep) can be attained; this new rate can be up to one order of magnitude faster than secondary creep (Steinemann, 1958).

In addition to the so-called Andrade creep, the transient creep includes an important anelastic contribution, probably produced by the dislocation motion at the sub-boundaries or the dislocation pile-ups (Duval, 1978).

For secondary creep, the strain-rates $\dot{\epsilon}_{ij}$ vary with the deviatoric stresses τ_{ij}' , with the relationship

$$\dot{\epsilon}_{ij} = \frac{B}{2} \tau^{n-1} \tau_{ij}', \quad (1)$$

where τ is the effective shear stress defined by: $\tau^2 = \frac{1}{2} \sum_{ij} (\tau_{ij}')^2$ and B is a constant. For stresses greater than one bar, the exponent n is about three and creep-rate is controlled by recovery processes (Duval, 1977), but for small stresses the creep-rate of fine-grained polycrystalline ice (grain size smaller than one millimeter) is controlled by diffusional processes (Duval, 1973).

The increase of strain-rate during tertiary creep is generally attributed to the formation of fabrics by recrystallization or deformation. Indeed, the plastic anisotropy of ice monocrystals is very important. The deformation of single crystals of ice occurs almost exclusively by glide on basal planes perpendicular to the optic axes (*c*-axes). In simple shear, the majority of new crystals introduced by the dynamic recrystallization have their *c*-axes oriented for basal glide (Steinemann, 1958). According to this author, more than 70% of crystals have their basal planes parallel to the permanent shear plane. So, tertiary creep is around one order of magnitude faster than secondary creep.

Lile (1978) has shown that the effect of anisotropy on the flow of ice is important. According to Russell-Head and Budd (1979), the shear strain-rates of glacier ices with multiple-maxima fabrics are of the same order of magnitude as those of randomly oriented polycrystalline ices, but the shear strain-rates of ices with basal planes well aligned near the permanent shear plane are typically three to five times the corresponding shear strain-rates of isotropic ices.

However, as Jonas and Müller (1969) pointed out, the increase of strain-rate during tertiary creep is not always due to a change of fabric. Thus, the fluctuations of strain-rate observed by Duval (1972) seem to be induced by periodic recrystallization processes, that is, to cycles of recrystallization followed by cycles of strain hardening. These processes of recrystallization occur simultaneously with the processes of recovery.

In the present study, polycrystalline ice samples were subjected to different states of stress with flow conditions similar to those found in glaciers. The tertiary creep was specially analysed using methods designed to examine changes in texture and fabric. The experimentally-produced fabrics were compared with natural fabrics of glacier ice and with theoretical fabrics produced by recrystallization or deformation.

EXPERIMENTAL METHODS

Apparatus

Two viscometers of the same type as those used by Steinemann (1958) and Kamb (1972) were built. With the first apparatus, the deformation experiments were only performed in simple shear (Duval, unpublished). The samples, in the shape of a hollowed-out cylinder (external diameter, 55–90 mm; internal diameter, 22–30 mm; height, about 100 mm), were subjected to an axial torsion whose moment had a constant value. The experiments were carried out at temperatures between -1 and -2°C . The torsional strains of the specimen were measured using a rotary variable resistor. The smallest strain that could be detected was equal to 1.3×10^{-5} .

With the second viscometer, the deformation was produced by subjecting the cylindrical specimen to combined torsion and axial compression (Duval, unpublished). The ice samples

(external diameter, 90 to 100 mm; internal diameter, about 30 mm; height, about 130 mm) were also fastened to toothed grips. The torsion-compression experiments were conducted at temperatures of $-0.10 \pm 0.02^\circ\text{C}$. The torsional and axial strains were measured by two linear variable differential transformer transducers (L.V.D.T.). The sensitivity of these strain measurements was approximately 10^{-5} .

The shear-stress variation across the cylinder depends on the ice flow law. In torsion-compression, the shear stress varies as well as the axial stress (Duval, unpublished). In pure torsion, the shear stress τ is proportional to $r^{1/n}$, where r is the radial distance from the torsion axis. The shear stress was calculated by assuming the validity of the law (1) with $n = 3$. The values quoted were calculated for the outer surface of the cylinder. The axial stress was calculated directly from the measurement of the applied load. The effect of the torsion on the axial stress was not taken into account. In the same way, the shear strain-rate was also calculated for the outer surface of the specimen.

Artificial ice samples

The artificial ice samples were prepared by saturating snow with distilled water and by freezing the mixture at -10°C . These ice specimens are slightly bubbly and have a density varying between 0.88 and 0.90 Mg/m³. The mean grain-size varied between 1 and 5 mm². This technique was used to produce fine-grained, homogeneous, and isotropic ice.

Natural ice samples

The natural samples came from a drilling carried out through the whole thickness of the glacier of the Vallée Blanche (French Alps). Only ices at depths of 50 and 171 m were studied. These samples, like artificial ices, contained air bubbles. The grain-size was approximately 8 mm for sample VB 50 and 15 mm for VB 171.

The initial fabrics of the natural ice specimens were studied by Fabre (1973). For VB 50, the optic axes were grouped round two maxima separated by 50° and symmetrically disposed about the specimen axis. For VB 171, the optic axes were grouped round four diamond-shaped maxima whose centre is approximately 45° from the specimen axis. The fabrics of both VB 50 and VB 171 samples are shown in Figure 1. It is important to note that the fabric pattern of natural glacier ice samples does not conform to the rotational symmetry of the tests in torsion and torsion-compression.

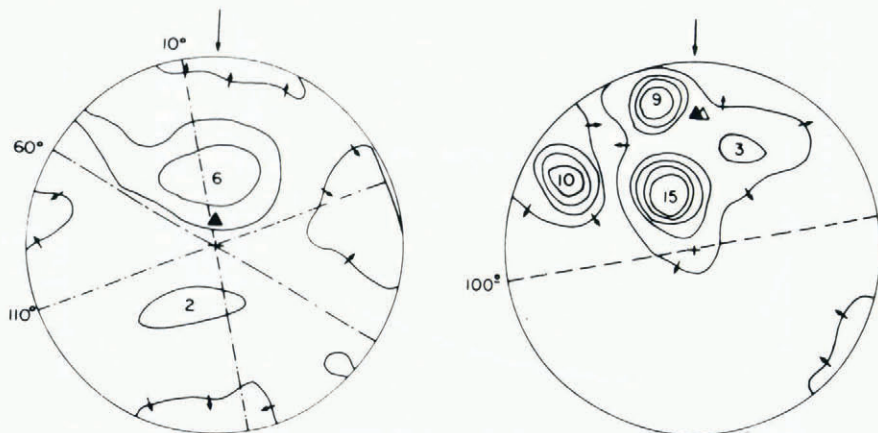


Fig. 1. *c*-axis fabrics of natural ice samples from Vallée Blanche (French Alps). The centre of the diagram corresponds to the vertical direction (torsion axis for deformation tests), from Fabre (1973).
a (left). Depth: 54.25 m, 133 crystals; contour lines for densities of 2, 4, and 6% of the points in 1% of the area.
b (right). Depth: 171 m, 88 crystals; contour lines for densities of 3, 6, 9, 12, and 15% of the points in 1% of the area.

Fabric measurement

At the end of each experiment the ice sample was immediately cooled to -16°C in order to avoid post-tectonic recrystallization. The thin sections studied were cut along mostly radial planes parallel to the cylinder axis. In these planes, the stress axes have everywhere the same orientation; the same is true for planes perpendicular to the radial direction provided that the width of the cross-section is small with regard to the diameter of the sample. The orientation of *c*-axes was measured on a universal stage. Measured *c*-axis inclinations were corrected in order to take air-ice refraction into account and plotted in equal-area Schmidt projection. The fabrics were shown by density curves. For each diagram a counter whose area is 1% of projection area was used.

CREEP CURVES AND FINAL FABRICS

Simple shear

Figure 2 shows a creep curve obtained at -1.0°C with an isotropic artificial ice. After a reduction due to the transient creep, the strain-rate passes through a minimum, then after several successive accelerations, stabilizes around a value equal to ten times that of the secondary creep. The final fabric is shown in Figure 3. The *c*-axes are located near the two poles of the planes of maximum shearing stress.

Figure 4 shows two creep curves obtained with two glacier ices (VB 50 and VB 171) at -1.0°C . With VB 50, the secondary creep continues to a total shear strain of 2% and is followed by the tertiary creep for which the creep-rate increases up to the end of the experiment. With VB 171 a continual increase in tertiary creep-rate is not found, but small oscillations in the creep-rate appear.

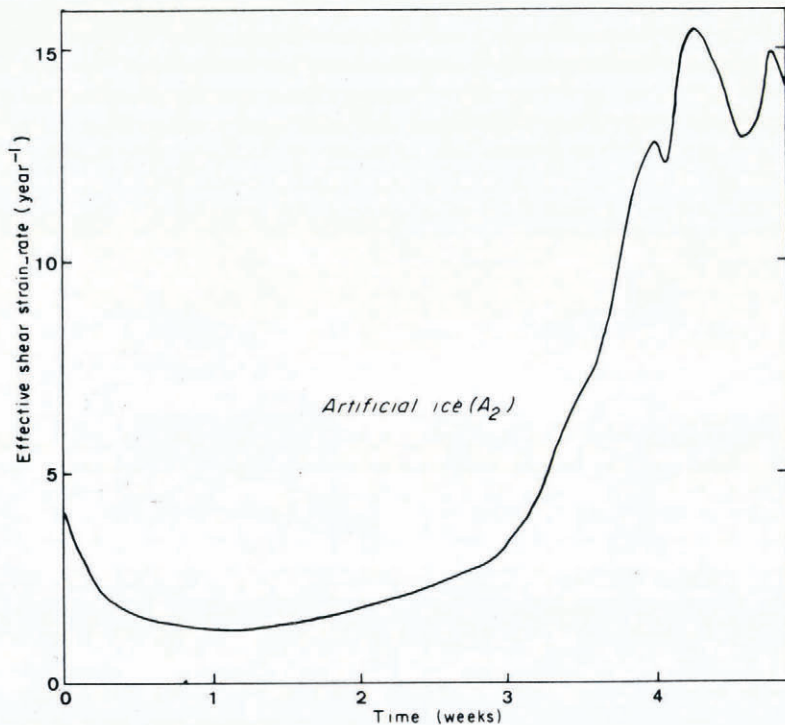


Fig. 2. Effective shear strain-rate versus time for a creep test performed in torsion. Artificial ice sample (A_2). $\tau = 2.50 \text{ bar}$, temperature $T = -1.0^{\circ}\text{C}$.

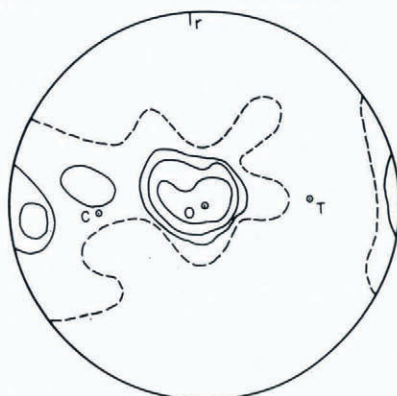


Fig. 3. c -axis fabric of specimen A2 after deformation in torsion. The contours are at densities of 2, 4, 6, and 8% in 1% of the area. C (compression), T (tension), and r are the axes of principal stresses. \circ is the axis of torsion. Total strain: 44%; number of c -axes measured: 106.

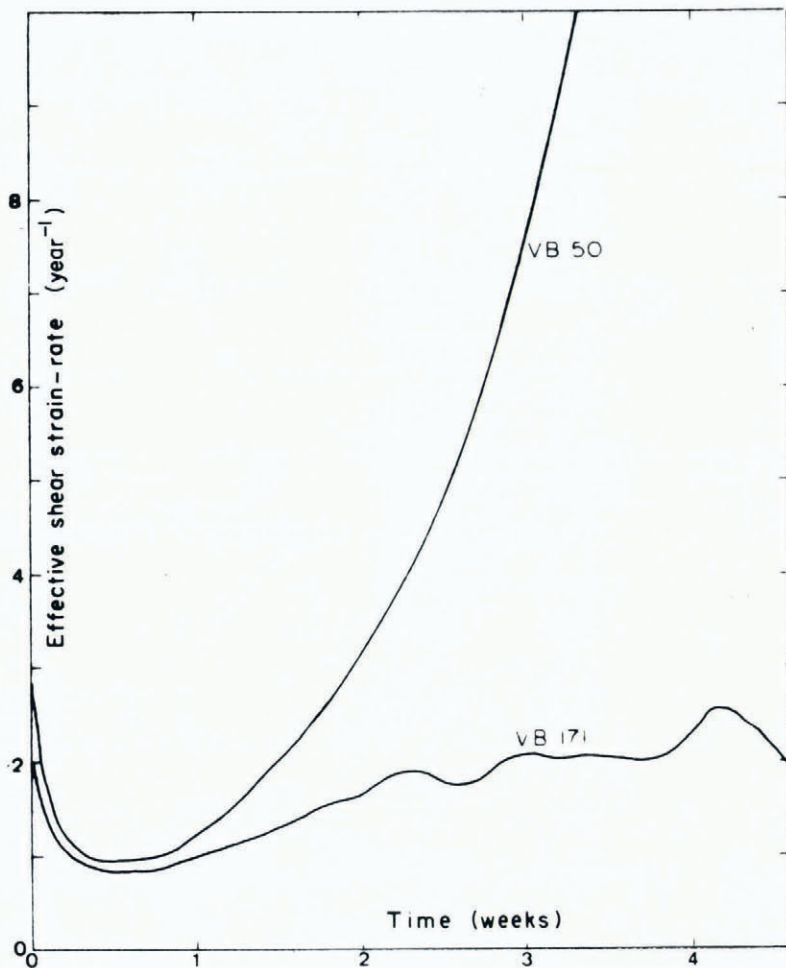


Fig. 4. Effective shear strain-rate versus time for a creep test performed in torsion. Natural ice samples: τ (VB 50) = 3.0 bar; τ (VB 171) = 2.7 bar; temperature T = -1.0°C .

As with the artificial sample mentioned earlier, the *c*-axis fabric of sample VB 50 which developed during deformation consisted of two strong maxima located near the two poles of the planes of maximum shear stress (Fig. 5). Unlike VB 50, the initial four-maximum fabric of VB 171 was found to be unchanged after deformation to a strain of about 16%.

A two-maximum fabric was obtained with another artificial ice sample when deformed to a shear strain of 45% (Fig. 6), but for this sample the stronger maximum is located near the pole of the permanent shear plane whereas the second maximum is situated between the principal direction of compression and the normal to the second plane of maximum shear stress. For this experiment, the shear stress was 3.3 bars during the first 13 and then 2.4 bars up to the end of the experiment. At the completion of the test, the tertiary creep-rate was roughly constant and its value was only equal to three times that of the secondary creep.

Torsion-compression

Figures 7 and 8 show the *c*-axis fabric for four artificial ice samples after deformation in torsion-compression at -0.10°C . Tests were carried out by applying the compressive stress and the torsion simultaneously. A three- or four-maximum fabric is found according to the values of the normal stress σ and the shear stress τ . In Figure 7, the *c*-axes are grouped round

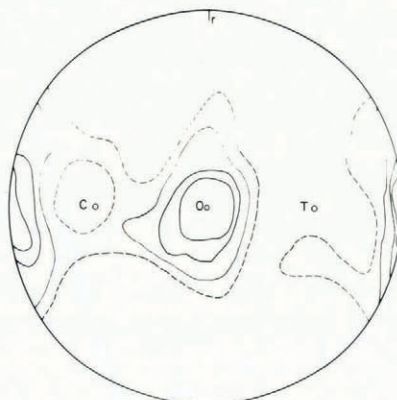


Fig. 5. *c*-axis fabric of specimen VB 50 after deformation in torsion. The contours are at densities of 1, 2, 4, and 6% in 1% of the area. Total strain: 24%; number of *c*-axes measured: 140. Symbols are defined in the caption to Figure 3.

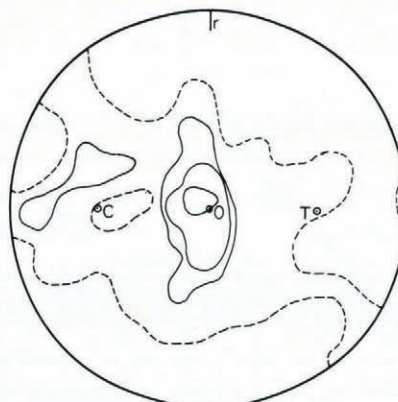


Fig. 6. *c*-axis fabric of specimen A3 after deformation in torsion. The contours are at densities of 0.5, 1, 2, 5, and 10% in 1% of the area. Total strain: 45%; number of *c*-axes measured: 144. Symbols are defined in the caption to Figure 3.

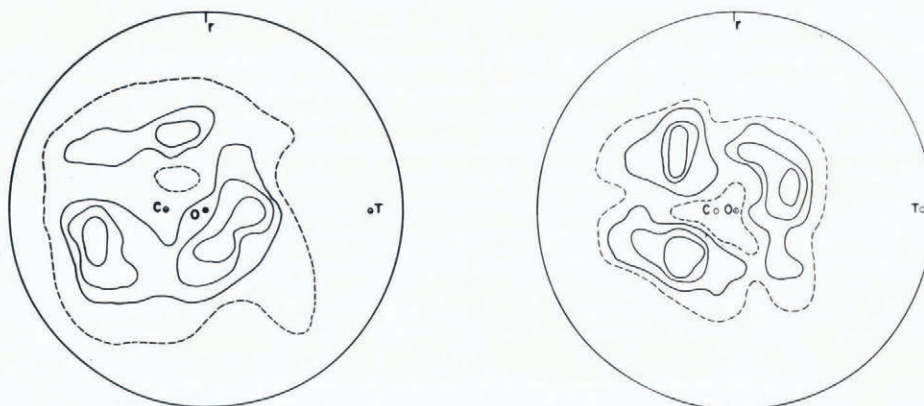


Fig. 7. c -axis fabrics of artificial ice samples after deformation in torsion-compression at -0.10°C . Symbols are defined in the caption to Figure 3.

a (left). TC A2 specimen. The contours are at densities of 0.5, 2, 4, and 6% in 1% of the area. Total strain in torsion: 14%; total strain in compression: 15%; number of c -axes measured: 245; shear stress τ : 1.85 bar; axial stress σ : 5.7 bar.

b (right). TC A1 specimen. The contours are at densities of 0.5, 2, 6, and 10% in 1% of the area. Total strain in torsion: 18%; total strain in compression: 26%; number of c -axes measured: 120; τ = 1.40 bar and σ = 6.0 bar.

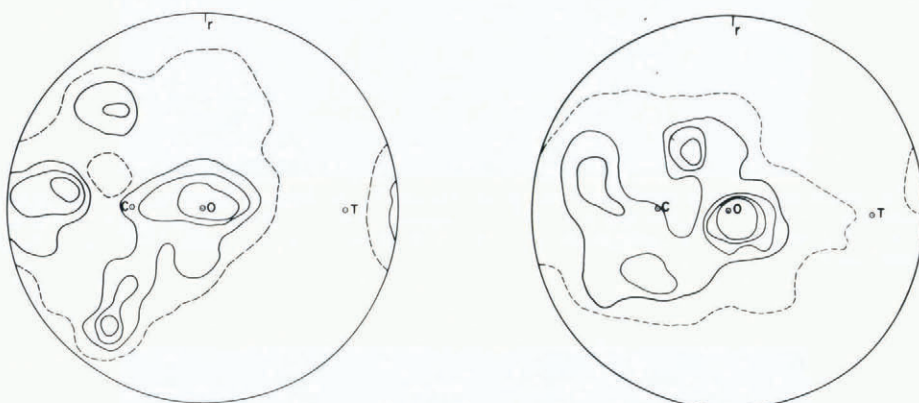


Fig. 8. c -axis fabrics of artificial ice samples after deformation in torsion-compression at -0.10°C . Symbols are defined in the caption to Figure 3.

a (left). TC A3 specimen. The contours are at densities of 0.5, 2, 4, and 6% in 1% of the area. Total strain in torsion: 13%; total strain in compression: 4.5%; number of c -axes measured: 215; τ = 2.2 bar and σ = 2.4 bar.

b (right). TC A4 specimen. The contours are at densities of 0.5, 2, 4, 6, and 8% in 1% of the area. Total strain in torsion: 25%; total strain in compression: 8%; number of c -axes measured: 241; τ = 2.8 bar and σ = 2.7 bar.

three maxima which are approximately the vertices of an equilateral triangle centred on the principal direction of compression. In Figure 8, the c -axes are grouped round four maxima arranged at the corners of a diamond-shape quadrangle centred again on the principal direction of compression. The statistical significance of preferred orientation was tested for the fabrics showed in Figures 7b and 8a by the methods given by Vallon (unpublished). For the fabric showed in Figure 7b, the contours were significant from a density of 8% per 1% of the area. So, the three-maxima fabric is probably real. For the fabric showed in Figure 8a, the contours were significant from a density of 5%. So, only three maxima would be significant. However, the four-maxima fabric is probably real on symmetry grounds.

Textural changes during flow

Figures 9 and 10 show the texture of the two samples of Figures 7 and 8 after deformation in torsion-compression. The thin sections were cut immediately after the experiments in planes containing the axis of compression stress and perpendicular to planes of maximum shear stress. The shape and the size of grains were altered during the flow. New crystals were formed with extensive grain-boundary migration. In spite of small differences in applied stresses, the crystal size varies inversely with the stress. Steinemann (1958) and Kamb (1972) found similar results in their study. Some crystals show sub-boundaries roughly parallel to the *c*-axis; they are probably formed by edge basal dislocations (tilt boundaries).



Fig. 9. Thin-section photograph of crystalline texture of ice specimen TC A2 between crossed polaroids after deformation in torsion-compression. $\tau = 1.85$ bar and $\sigma = 5.7$ bar; dimensions of the thin-section: 8 cm \times 4.5 cm. The torsion axis was parallel to the direction containing the largest dimension of the thin section. The radial direction was perpendicular to the thin section.



Fig. 10. Thin-section photograph of crystalline texture of ice specimen TC A4 between crossed polaroids after deformation in torsion-compression. $\tau = 2.8$ bar and $\sigma = 2.7$ bar; dimensions of the thin section: 8 cm \times 4.6 cm. The torsion axis was parallel to the direction containing the largest dimension of the thin-section. The radial direction was perpendicular to the thin section.

Interpretation of experimentally produced fabrics

The development of preferred orientation of *c*-axes in ice, which occurs during hot working, has been investigated for more than 20 years (Shumskiy, 1958; Kamb, 1959). These authors considered the formation of recrystallization fabrics. The preferred orientations developed by plastic flow were not taken into account. From Kamb (1959), the driving force of syntectonic recrystallization is attributed to differences in elastic strain energy between deformed crystals in a non-hydrostatic stress field. The experimentally-produced fabrics are incompatible with this thermodynamic theory.

Indeed, in simple shear and torsion-compression the more stable crystals are those whose basal planes are nearly parallel to the planes of maximum shear stress. In addition, the stress-induced recrystallization model proposed by Kamb (1959) excludes plastic flow by dislocation motion. According to Kamb (1972), it is likely that the stress is not homogeneous in the polycrystalline aggregate because of intracrystalline plastic anisotropy. The ice crystals whose basal planes are parallel to the planes of maximum shearing stress are the least stressed and, consequently, are more stable, as indicated by the thermodynamic theory discussed previously.

An alternative suggestion is to explain the fabrics as being formed by the strain-induced recrystallization process (Nicolas and Poirier, 1976). The driving force for this recrystallization process is provided by differences in stored plastic strain energy (dislocation energy). As discussed previously, the grains oriented for basal gliding are the least stressed. Transition bands (or deformation bands) must develop in the more highly stressed crystals and the sub-grain size must be greater in the least stressed crystals (Weertman, 1973). If a grain boundary or a highly misoriented sub-boundary (boundaries of transition bands) separates regions with subgrains of different size, large subgrains must grow at the expense of small subgrains by strain-induced boundary migration (Bailey and Hirsch, 1962). These recrystallization processes may explain the two-maxima fabrics developed in simple shear shown in Figures 3 and 5, but, in Figure 6, the two-maxima fabric is not compatible with the stress state. One maximum is always normal to the first plane of maximum shear stress, whereas the other is situated between the principal direction of compression and the normal to the other plane of maximum shear stress. So, in order to explain the fabric shown in Figure 6, the deformation state must be taken into account. The fabric displays the difference between a pure shear deformation and a simple shear deformation. The stronger maximum is always normal to the permanent shear plane and its position is stable towards orientation processes induced by plastic flow. The maximum strain achieved in the present study was only 45%, so intracrystalline glide cannot be the single process of fabric formation, but is rather a complementary process which becomes important when the syntectonic recrystallization slows down.

By superposing a compressive stress in simple shear (torsion-compression tests), we prevent any permanent shear plane. The three maxima shown in Figure 7 are, as in simple shear, in positions of high shear stress. To produce any homogeneous deformation by dislocation glide alone without change of volume, it is necessary for at least five independent glide systems to be operative. Two only are available by basal glide, and so other deformation modes must be initiated in torsion-compression or, as proposed by Lliboutry (1964), several preferred orientations of *c*-axis should attenuate internal stresses and make the deformation more homogeneous.

Another possibility is that the final fabric is determined by the migration velocity of grain boundaries as a function of the relative orientations of the growing grain and the grain which is disappearing. Recrystallization and grain-boundary migration were occurring during deformation as indicated by the textures shown in Figures 9 and 10. Matsuda and Wakahama (1978) have measured the orientation of both *a*- and *c*-axes in polycrystalline ice with four-maxima fabrics from Antarctica. These authors concluded that ice crystals were in twinning relationships and suggested that the multiple-maximum diamond fabrics are induced by

mechanical twinning. It is also possible that annealing twins are formed during grain-boundary migration, as observed in many materials (Christian, 1965). It is likely that the special boundaries of the near-coincidence site type migrate more readily than other boundaries (Pumphrey, 1976). So, syntectonic recrystallization would produce grains with *c*-axes oriented for basal glide. The final fabric, however, would be determined by the orientation of the grains which grow fastest.

*Comparison with *c*-axis fabrics of glacier ice*

The typical *c*-axis fabric of glacier ice consists of four maxima at the corners of a diamond-shaped figure (Rigsby, 1951). According to Kamb (1972), maxima are clustered around the pole of the shear plane. But, according to Vallon (unpublished), the *c*-axis fabric of glacier ice from surface samples of Mer de Glace consists of three or four maxima clustered round the principal direction of compression. These conflicting results may arise from lack of knowledge of the stress state in glaciers, but the maxima positions of the experimentally-produced fabrics with regard to the stress configuration are compatible with the results given by Vallon (unpublished) rather than with those of Kamb (1972).

To explain the difference between glacier-ice and experimentally-produced fabrics, Kamb (1972) surmises that there exists a second mechanism which can control the *c*-axis orientations, but which becomes operative only at strains higher than 100%. In the accumulation area of Vallée Blanche the four-maxima fabrics appear at a strain of about 60% (Vallon and others, 1976). As discussed previously, stable fabrics can be formed at small strains provided that syntectonic recrystallization proceeds very quickly. If the recrystallization processes occur only with difficulty, the influence of plastic flow becomes important and final fabrics are developed at high strains. Such is the case for fabrics observed by Hudleston (1977) in a shear zone at the margin of the Barnes Ice Cap. In the centre of the shear zone, where the shear strain is at a maximum (total strain 500 to 800%), the fabric consists of a single strong maximum around the pole of the permanent shear plane whereas a two-maxima fabric is found for the margin of the shear zone where the shear strain is much smaller. In the same way, the fabrics of glacier ice with morainic debris at G1 site, Antarctica consists also of a strong maximum probably located near the pole of the permanent shear plane (Lorius and Vallon, 1967). As was shown by Gow and Williamson (1976), particles can inhibit syntectonic recrystallization and crystal growth.

Creep-rate in relation to fabrics and recrystallization processes

Creep-rate was found to depend on fabric. The tertiary creep-rate of the artificial sample deformed in simple shear was about ten times that of secondary creep (Fig. 2). The same result was obtained with the VB 50 sample, but, for this sample, the steady state was not reached (Fig. 4). As shown in Figures 3 and 5, the great majority of crystals were orientated for basal glide. Only an increase by a factor of three was found for the artificial sample whose fabric is showed in Figure 6 and for sample VB 171. For these samples, the fabrics were not as favourable for deformation as the fabrics of Figures 3 and 5. These results are in accordance with the conclusions given by Lile (1978) about the effect of anisotropy on the creep of polycrystalline ice. In torsion-compression, the tertiary creep-rates were always two or three times higher than the secondary creep-rates. The role of a permanent shear plane in simple shear should be examined when anisotropy is included as a flow variable.

The increase of strain-rate after secondary creep does not arise solely from the formation of new fabrics. Indeed with sample VB 171, no change of *c*-axis orientation was found after deformation. The softening processes associated with dynamic recrystallization were probably at the origin of the increase in creep-rate during tertiary creep (Jonas and Müller, 1969;

Duval, 1972). These recrystallization processes must occur during the deformation of ice in temperate glaciers. So, the effect of dynamic recrystallization must be taken into account in the flow laws of polycrystalline ice strained near the melting point.

CONCLUSIONS

In simple shear, the experimentally-produced fabrics consist of two maxima; one is always at the pole of the permanent shear plane, whereas the other is between the pole of the second plane of maximum shear stress and the principal direction of compression. Two-maxima fabrics can be stable if the syntectonic recrystallization is the principal mechanism of fabric formation. The one-maximum fabrics, as observed in the shear zones of glaciers, are developed after very high strains. These fabrics are probably produced by plastic flow even if the syntectonic recrystallization accompanies the deformation. The three- or four-maxima fabrics developed in torsion-compression seem to be of the same type as the typical multiple-maxima fabrics of glacier ice.

Only fabrics developed in simple shear appear to influence the creep-rate. Dynamic recrystallization processes must be responsible for the increase in strain-rate by up to three times the secondary creep-rate during tertiary creep.

ACKNOWLEDGEMENTS

I am most grateful to Professor L. Lliboutry for his guidance in this work and for providing advice and criticism. I wish to acknowledge A. Chaillou's help in the experiments and the technical assistance of D. Donnou, C. Girard, and L. Philippe. I thank the Centre National de la Recherche Scientifique for financial support.

MS. received 28 November 1974 and in revised form 4 July 1979

REFERENCES

- Bailey, J. E., and Hirsch, P. B. 1962. The recrystallization process in some polycrystalline metals. *Proceedings of the Royal Society of London, Ser. A*, Vol. 267, No. 11, p. 11-30.
- Christian, J. W. 1965. *The theory of transformations in metals and alloys*. Oxford, etc., Pergamon Press.
- Duval, P. 1972. Fluage et recristallisation dynamique de la glace polycristalline. *Comptes Rendus Hebdomadaires des Séances de l'Académie des Sciences* (Paris), Sér. D., Tom. 275, No. 3, p. 337-39.
- Duval, P. 1973. Fluage de la glace polycristalline pour les faibles contraintes. *Comptes Rendus Hebdomadaires des Séances de l'Académie des Sciences* (Paris), Sér. A, Tom. 277, No. 14, p. 703-06.
- Duval, P. 1977. Lois de fluage transitoire ou permanent de la glace polycristalline pour divers états de contrainte. *Annales de Géophysique*, Tom. 32, No. 4, 1976, p. 335-50.
- Duval, P. 1978. Anelastic behaviour of polycrystalline ice. *Journal of Glaciology*, Vol. 21, No. 85, p. 621-28.
- Duval, P. Unpublished. Fluage et recristallisation des glaces polycristallines. [D. d'Etat thesis, Université Scientifique et Médicale de Grenoble, 1976.]
- Fabre, B. Unpublished. Pétrographie structurale de la glace profonde. Vallée Blanche Supérieure, Massif du Mont Blanc. [Thesis, 3^e cycle, Université de Grenoble, 1973.]
- Glen, J. W. 1955. The creep of polycrystalline ice. *Proceedings of the Royal Society of London, Ser. A*, Vol. 228, No. 1175, p. 519-38.
- Gow, A. J., and Williamson, T. C. 1976. Rheological implications of the internal structure and crystal fabrics of the West Antarctic ice sheet as revealed by deep core drilling at Byrd Station. *U.S. Cold Regions Research and Engineering Laboratory. Report 76-35*.
- Hudleston, P. J. 1977. Progressive deformation and development of fabric across zones of shear in glacial ice. (*In* Saxena, S., and Bhattacharji, S., ed. *Energetics of geological processes*. New York, Springer-Verlag, p. 121-50.)
- Jonas, J. J., and Müller, F. 1969. Deformation of ice under high internal shear stresses. *Canadian Journal of Earth Sciences*, Vol. 6, No. 4, Pt. 2, p. 963-68.
- Kamb, W. B. 1959. Theory of preferred crystal orientation developed by crystallization under stress. *Journal of Geology*, Vol. 67, No. 2, p. 153-70.
- Kamb, W. B. 1972. Experimental recrystallization of ice under stress. (*In* Heard, H. C., and others, ed. *Flow and fracture of rocks*, edited by H. C. Heard, I. Y. Borg, N. L. Carter, and C. B. Raleigh. Washington, D.C., American Geophysical Union, p. 211-41. (Geophysical Monograph 16.))

- Lile, R. C. 1978. The effect of anisotropy on the creep of polycrystalline ice. *Journal of Glaciology*, Vol. 21, No. 85, p. 475-83.
- Lliboutry, L. A. 1964-65. *Traité de glaciologie*. Paris, Masson et Cie. 2 vols.
- Lorius, C., and Vallon, M. 1967. Étude structurographique d'un glacier antarctique. *Comptes Rendus Hebdomadiers des Séances de l'Académie des Sciences* (Paris), Sér. D, Tom. 265, No. 4, p. 315-18.
- Matsuda, M., and Wakahama, G. 1978. Crystallographic structure of polycrystalline ice. *Journal of Glaciology*, Vol. 21, No. 85, p. 607-20.
- Nicolas, A., and Poirier, J. P. 1976. *Crystalline plasticity and solid state flow in metamorphic rocks*. New York, Wiley-Interscience.
- Pumphrey, P. H. 1976. Special high angle grain boundaries. (In Chadwick, G. A., and Smith, D. A., ed. *Grain-boundary structure and properties*. New York, Academic Press, p. 139-200.)
- Rigsby, G. P. 1951. Crystal fabric studies on Emmons Glacier, Mount Rainier, Washington. *Journal of Geology*, Vol. 59, No. 6, p. 590-98.
- Russell-Head, D. S., and Budd, W. F. 1979. Ice-sheet flow properties derived from bore-hole shear measurements combined with ice-core studies. *Journal of Glaciology*, Vol. 24, No. 90, p. 117-30.
- Shumskiy, P. A. 1958. The mechanism of ice straining and its recrystallization. *Union Géodésique et Géophysique Internationale. Association Internationale d'Hydrologie Scientifique. Symposium de Chamonix, 16-24 sept. 1958*, p. 244-48. (Publication No. 47 de l'Association Internationale d'Hydrologie Scientifique.)
- Steinemann, S. 1958. Experimental Untersuchungen zur Plastizität von Eis. *Beiträge zur Geologie der Schweiz. Geotechnische Serie. Hydrologie*, Nr. 10.
- Vallon, M. Unpublished. Contribution à l'étude de la Mer de Glace. [D. d'État thesis, Université de Grenoble, 1967.]
- Vallon, M., and others. 1976. Study of an ice core to the bedrock in the accumulation zone of an Alpine glacier, by M. Vallon, J.-R. Petit, and B. Fabre. *Journal of Glaciology*, Vol. 17, No. 75, p. 13-28.
- Weertman, J. 1973. Creep of ice. (In Whalley, E., and others, ed. *Physics and chemistry of ice: papers presented at the Symposium on the Physics and Chemistry of Ice, held in Ottawa, Canada, 14-18 August 1972*. Edited by E. Whalley, S. J. Jones, L. W. Gold. Ottawa, Royal Society of Canada, p. 320-37.)